Ocean and Coastal Management 208 (2021) 105635

Contents lists available at ScienceDirect

Ocean and Coastal Management

journal homepage: www.elsevier.com/locate/ocecoaman

Efficiency of Chinese ECA policy on the coastal emission with evasion behavior of ships

Zhijia Tan [a], Haiyan Liu [a], Shuai Shao [a,*], Jiaguo Liu [a], Jihong Chen [b]

[a] School of Maritime Economics and Management, Dalian Maritime University, 116026 Dalian, PR China
[b] College of Management, Shenzhen University, 518061 Shenzhen, PR China

ARTICLE INFO

Keywords:
Emission control area
AIS data
Evasion behavior
Emission reduction

ABSTRACT

As the main component of international transportation, the shipping industry cannot be underestimated in pollutant emissions. To control the emission of pollutants, IMO and the major countries have designed ECA to limit ships' emission in the offshore area. The implementation of ECA has a direct impact on the ship's cost. Therefore, this paper studied how the ship's behavior changes under ECA policy. Furthermore, we simulated the ship's evasion trajectory under different ECA policies using AIS data. Meantime, the change of ship cost and emission reduction under different policies is analyzed. We found that the distorted emission reduction is increasing first and decreasing with the ECA boundary moving far away from the coastline. The saved cost by evasion behavior has the same variation trend. Furthermore, the emission reduction efficiency related to the increase in ship's operating cost has a peak value with the distance of ECA boundary moving. This study could help the government to evaluate and design ECA policy.

1. Introduction

1.1. Research background

Over 80 percent of global trade by volume and more than 70 percent of its value being carried onboard ships and handled by seaports worldwide (UNCTAD, 2017). Compared with last year, the growth rate of container throughput ports has dropped considerably caused by the COVID-19 and trade disputes (UNCTAD, 2020). The development of Container transportation in China is still the center of gravity and the foundation of stable global development. In the meantime, with the generator of internal trade benefited by shipping, there have caused damage to the ocean system, inland river system, and air system. The emission generated by coastline port or ships also caused colossal destruction to the environment and economy (Wang et al., 2020), such as oily sewage of port's equipment, sanitary sewage, and transportation accidents.

Many worldwide governments have delimited the Emission Control Areas (ECAs) to reduce the coastal area's pollution. The emission of pollution is limited strictly when the ship sails in the ECA. The IMO first discussed the issue of air pollution in 1988 (Carr and Corbett, 2015). However, the first ECA was not implemented until 2005 in the Baltic. The North Sea and North American ECAs followed in 2006 and 2012, respectively (IMO, 2021). China's total import and export volume ranks first globally, which attaches great importance to marine spatial planning (Yu et al., 2020) and ships' emission. By 2020, China still accounts for nearly half of the world's top 20 container ports and seven top 10 container ports (WSC, 2021). China's government has published the ECA policy to control the ships' emission from 2019. The ECA boundary from the coastline of North American is about 24 nm. However, the Chinese ECA distance is 12 nm. This distance is controversial because it is too close to shore. China's government has published the emission regulation within ECA is required 0.5%m/m from 2019 (MOT, 2018).

After ECA regulation is published, there have three choices for the ship to reply with ECA regulation (Fagerholt et al., 2015). The first and widely used way is changing fuels. The ship burns Marine Gas Oil (MGO) in ECA to satisfy the emission regulation and changes to burn Heavy Sulfur Fuel Oil (HSFO) outside the ECA, because MGO is more expensive than HSFO. The ECA policy would result the ship to choose to sail near the ECA boundary burning HSFO, which generates extensive pollution along the ECA boundary. The oil change strategy is the most popular among shipowner. The second choice is to install the scrubber, which could filter the emission gas. However, this way is not suiting for all types of ships. The last choice is to burn Liquefied Natural Gas (LNG) (Mollenbach et al., 2012; Pawlak, 2015). LNG technology uses liquefied natural gas as fuel, eliminating SO_x emissions and reducing NO_x and

* Corresponding author.
E-mail addresses: zjatan@dlmu.edu.cn (Z. Tan), dmulhy@163.com (H. Liu), shuaishao@dlmu.edu.com (S. Shao), liujiaguo@gmail.com (J. Liu), cxjh2004@163.com (J. Chen).

https://doi.org/10.1016/j.ocecoaman.2021.105635
Received 7 January 2021; Received in revised form 16 March 2021; Accepted 21 March 2021
Available online 8 April 2021

PM emissions simultaneously. However, it requires a large investment to transform new engines, so fewer shipping companies choose to use LNG technology. In conclusion, the ECA policy could reduce pollution emissions in the ECA. On the other hand, this would lead to an increase in the operation cost of ships. So, how to evaluate the ship's emission reduction and the ship's cost increase accurately is essential for the government to design a reasonable ECA policy.

1.2. Main contribution

The motivation of the paper is to develop the methodology to evaluate the efficiency of ECA policy with the consideration of ships' evasion behavior. We first theoretically investigated the evasion behavior of ships in the sense of minimization of the total operation cost. Inside ECA, a ship must burn expensive MGO, while, outside ECA, a ship can use heavy oil with a lower price. A ship would save its operation cost with the evasion behavior or to sail outside ECA. By assuming a liner ECA boundary and a two-port shipping network, we derived the sufficient condition for a ship to adopt evasion behavior. Then, according to the condition, we built the simulation method for different ships and trajectories. The evasion behavior of ships is incorporated in the evaluation of ECA policy.

The main contribution is three-fold. First, we proposed the mathematical model in the sense of the total operation cost with and without evasion behavior to analyze the sailing trajectories of coastal ships under the ECA policy. Second, by incorporating the evasion behavior of ships, the paper provided evacuation method of ECA policy and investigated the emission effect of the evasion behavior by simultaneously considering the operation cost and quantity of air pollutants. The proposed method would be more explicit and helpful for the local government to design the more efficient emission control area.

2. Literature review

One side of the literature investigating the emission control area has focused on the ship's decision under ECA policy to minimize the ship's operation cost. In order to save the cost of the ship under ECA policy, Fagerholt et al. (2015), Cariou et al. (2018),Peng et al. (2016) and Zhen et al. (2018) established the mixed-integer programming models to optimize the ship's sailing pattern. Zhen et al. (2018) and Cariou et al. (2018) focused on shipping network design using the heuristic algorithm. Fagerholt et al. (2015) and Freedman et al. (2017) aimed at ship's routing and speed optimization and found that ship operators prefer to pass by ECA boundary to sail. Otherwise, the speed of the ship in ECA is lower than sailing outside of ECA. Chen et al. (2017) revealed that the small ships are more inclined to re-route than big ships under ECA policy. The ECA is set to control the sulfur emission, but the CO_2 emissions will increase, which is caused by higher-speed out of ECA. Future, Ma et al. (2020a) proposed a multi-objective model to optimize ship routing and speed. In the same year, another work by Ma et al. (2020b) imported two categories to optimize the ship's route and speed simultaneously. Dong and Lee (2020) examined the dual environmental effects of ECA and Reduced Speed Zones (RSZs). Compared to the separate establishment of ECAs, joint regulations of ECAs and RSZs can lead to more SO_x emission reduction within it and less profit loss of the container ship utilizing differentiated operation. Except for re-designing the ship's routing and adjusting sailing speed, using MGO and installing scrubbers are the other two choices to decrease cost (Moore et al., 2018). Wan et al. (2019a) and Wan et al. (2019b) focused on the risk factors of maritime supply chains. The above mentioned studies mainly focused on ship network design or shipping pattern choice. Therefore, it is important to design heuristic algorithms or exact algorithms for the MIP model. The sailing trajectories of ships under ECA policy is seldom considered in those optimization problems.

Another line of research focused on the evaluate the emission reduction of ECA policy. The ECA is designed to reduce pollutant emission neighbor the coastline, and Viana et al. (2015) and Zhang et al. (2020) analyzed the ECA policy's benefit the environment and resident health. Shi et al. (2020) used AIS data in 2017 to investigate emissions reduction for different ship types, and the result showed the NO_x emissions not significantly changed under different ECA policies. On the other hand, the government has to trade-off industrial growth and environmental protection (Zheng et al., 2020). Jiang et al. (2020) constructed an evolutionary game model to analyze the balance between the government and shipping companies. A dynamic penalty is a practical approach to incentivizing the shipping company to fulfill the ECA policy. Okada (2019) incorporated an air pollutant model to evaluate ECA's size based on a one-dimensional linear city and a linear sea. Moreover, to reduce the port's emission, the government incentive using on-shore power replace of fuel to supply power to the auxiliary engine when ship berthing in the port. Peng et al. (2019) and Kong and Liu (2021) imported the greenhouse gas as an index to evaluate the port's efficiency, and a two-stage interaction model is established to measure the port city's sustainable ability. The above studies tended to investigate the emission reduction under the current policy, and the ship sailing behavior has not yet been considered. In fact, under the ECA policy, a coastal ship would adjust its trajectory to sail outside ECA which allows the ship to burn cheap heavy oil, but adds the sailing distance, simultaneously. The evasion behavior would distort the emission estimation of the ECA policy. It is necessary to develop evaluation method of the ECA policy with the explicit consideration of the ships' evasion behavior.

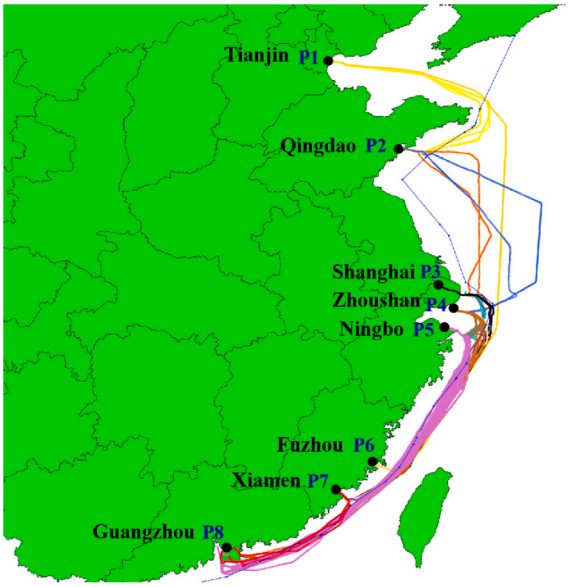

Fig. 1. Referred trajectories and ECA boundary.

Moreover, there have some researches focused on the effects of ECA regulations on fuel switching ships and the corresponding particular response strategies (sailing pattern and evasion strategy selection). To investigate the effect of the ECA on the strategic behavior of ships, Wang and Peng (2019) provided a simple geometric method to analyze the trajectory adjustment of a coastal ship traversing two given ports by applying the cost minimization model proposed by Ronen (1982) and Fagerholt et al. (2015). Their method follows two basic assumptions: the ECA boundary is a line, and the distance between any port and the boundary is identical. The two assumptions are quite ideal. The coastline is quite complicated, and the distances between ports and ECA boundary are not identical. Also, the irregular coastline results in the trajectories of ships is not a line. Furthermore, the ECA boundary is typically a piecewise line or curve. Fig. 1 shows the real trajectories and ECA boundary of China with 15 ships and over 100 trajectories

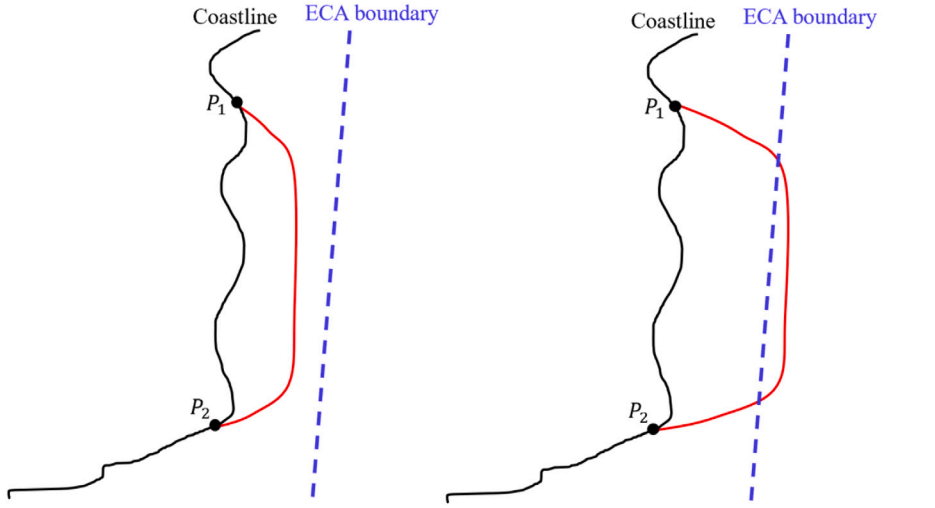

(a) The initial trajectory locates inside ECA (b) The initial trajectory passes through the outside ECA

Fig. 2. Graphical explanation of ports, ECA boundary and initial trajectory.

connecting eight ports with a one-year AIS data. This paper will extend the geometric method proposed by Wang and Peng (2019) to relax the two assumptions. Then, the revised geometric method is applied to assess the effect of China's ECA policy on the trajectory evasion strategy for the coastal ships. Li et al. (2020) got the evasion strategy by a mixed-integer non-nonlinear programming model to evaluate the ship's behavior under different port pair in North American ECA. However, mixed-integer nonlinear programming models are challenging to solve. The author using an ingenious enumeration method to get the evasion points in the ECA boundary. Different from Li et al. (2020), we demonstrated that the course angle is a particular value if the ship chooses to pass by, which could avoid solving the model frequently. Moreover, this paper proposed a general simulation method to simulate the ship's behavior under the given ECA policy.

The current paper considers the container ships sailing between two predetermined ports on the coastal area. We first theoretically investigated the evasion behavior of ships to minimize the total operation cost. We assume that a ship must burn expensive MGO inside ECA, but can use heavy oil with a lower price outside ECA. Therefore, the ship can sail outside ECA to trade-off its sailing distance and operation cost. In fact, the evasion behavior would increase the emission of coastal area and distort the efficiency of ECA policy. The aim of the paper is to derive the sufficient condition for a ship to adopt evasion behavior and provide the evaluation of ECA policy with consideration of the evasion behavior of ships.

The remainder of this paper is organized as follows. Section 3 describes our problem and investigates the evasion behavior of coastal cargo ships. The mathematic model formulations are also given in this Section. Section 4 develops the simulation analysis of the ship's behavior under different ECA boundary. Finally, concluding remarks are presented in Section 5.

3. Problem description and model formulations

Consider the coastal cargo ships traversing between two predetermined ports on the coastline, P and P'. The navigational area is separated into emission control area (ECA) and outside ECA. Only the Marine Gas Oil (MGO) with a higher price P_M is permitted in the ECA area, while the High Sulfur Fuel Oil (HSFO) with a lower price P_H is allowed outside ECA. To simplify our discussion, the ECA boundary Γ is assumed to be a line. Notations used in this paper are listed in Table 1.

Before ECA policy, the initial trajectory of a ship is denoted by $\mathcal{J}_0$. It must be pointed out that, for the practical consideration, the initial trajectory $\mathcal{J}_0$ would locate inside ECA or bypass the outside ECA. Fig. 2 provides a graphical explanation of ports, ECA boundary and initial trajectory. The initial trajectory $\mathcal{J}_0$ would completely locate inside ECA or passes through outside ECA, shown in Fig. 2(a) and (b), respectively. Hereinafter, we represent the two cases shown Fig. 2(a) and (b) correspondingly as cases (a) and (b). This figure only gives a general sailing pattern if the ship chooses sailing inside the ECA and outside the ECA. In the ship's actual sailing, its trajectory may be affected by the sea environment or condition such as ocean current, wave height, and wind velocity. These uncertain ocean conditions will directly affect the sailing speed of ships. A random variable related to the optimal sail speed could be imported to depict the actual speed affected by uncertain ocean conditions, which satisfies a Gaussian distribution with the mean near 0. In the simulation process, the adjusted trajectory only could sail outside of its original trajectory, which is a consideration of the natural ocean environment. Let l_0^E and l_0^{NE} denote the arc lengths inside and outside ECA. When the initial trajectory locates completely inside ECA, l_0^{NE} vanishes to zero. It is reasonable to assume that the initial trajectory $\mathcal{J}_0$ is optimal one with shortest length under safe consideration. Otherwise, with given sailing speed, $\mathcal{J}_0$ is not the optimal provided that a ship can find another shorter trajectory. The initial trajectory $\mathcal{J}_0$ can be estimated by the historical trajectories of the ship between the two ports.

After emission regulation, the trip cost of a ship surely increases. To reduce the negative effect to a ship, beside the speed adjustment, a ship would consider an evasion behavior or bypass the ECA. For an evasion behavior, we assume that the evasion trajectory is shifted to the right-hand side of the initial trajectory with a larger length. Furthermore, we assume that a ship cannot frequently enter and exit the ECA. That is to say, there are at most two intersections between the evasion trajectory and ECA boundary. In this case, a ship firstly sails inside ECA, then bypasses outside ECA, finally sails inside ECA and arrivals its destination. Denote $\mathcal{J}$ as the evasion trajectory, which is assumed to be a piecewise line and can be split into two segments inside and outside ECA with arc lengths l^E and l^{NE}, respectively.

3.1. Evasion behavior of coastal ships under emission regulation

According to the basic model proposed by Ronen (1982), the trip cost of a ship is the sum of the operation cost and the fuel cost. The former is related to the routine enpension and equals the production of the hourly operation cost and the trip time between the two ports.

Table 1
List of notations.

Notation	Description	Notation	Description
c_0	The ship's unit operation cost (USD/hour)	P_M	The price of MGO(USD/mt)
C_0	The total traversing cost of a ship	P_H	The price of HSFO(USD/mt)
v_0^E	The ship's sailing speed inside the ECA	F	The burn fuel ratio
v_0^{NE}	The ship's sailing speed outside the ECA	$\bar{v}$	The max speed of the ship
l_0^E	The sailing length inside the ECA	α	The scaling factor
l_0^{NE}	The sailing length outside the ECA	Γ	The ECA boundary

The latter is the production of the hourly fuel consumption and the trip time. A power-type function of sailing speed is adopted to capture the hourly bunker consumption of a ship (Wang and Meng, 2012; Meng et al., 2016; Tan et al., 2018). Without schedule constrain, the total cost of a ship traversing between ports P and P' without evasion behavior is the sum of the trip costs inside and outside ECA, namely,

$$C_0(v_0^E, v_0^{NE}) = c_o\left(\frac{l_0^E}{v_0^E} + \frac{l_0^{NE}}{v_0^{NE}}\right) + P_M F \frac{l_0^E}{v_0^E}\left(\frac{v_0^E}{\bar{v}}\right)^\alpha + P_H F \frac{l_0^{NE}}{v_0^{NE}}\left(\frac{v_0^{NE}}{\bar{v}}\right)^\alpha \tag{1}$$

where F is the fuel consumption of the ship per unit time (liter/hour); $\bar{v}$ is the maximal sailing speed (knots/hour); c_o is operation cost per unit time (USD/hour); v^E and v^{NE} are the sail speeds inside and outside ECA; α is the model parameter with $\alpha \geq 3$. The value of α comes from the Ronen (1982). In the model, α is the model parameter working on the ratio between ship operation speed and max speed. This parameter is used as a constant input model, with a greater than 2, usually 3. Note that, for the coastal ship, it is reasonable to measure time in hour since the trip time is not too long.

The optimal sailing speed before regulation for given lengths inside and outside ECA l_0^E and l_0^{NE} can be expressed as the minimization problem $\min_{v_0^E, v_0^{NE} \in [0,\bar{v}]} C_0(v_E, v_{NE})$. If an inner solution of the minimization problem can be achieved, with standard optimization method, we readily have

$$v_0^E = \bar{v}\left(\frac{c_o}{(\alpha-1)P_M F}\right)^{1/\alpha} \tag{2}$$

and

$$v_0^{NE} = \bar{v}\left(\frac{c_o}{(\alpha-1)P_H F}\right)^{1/\alpha} \tag{3}$$

Nota that, the optimal sailing speed v_0^E and v_0^{NE} are independent on the corresponding arc lengths l_0^E and l_0^{NE}. Substituting v_0^E and v_0^{NE} given by Eqs. (2) and (3) into Eq. (1), we get the total cost without evasion behavior

$$\begin{aligned} C_0 &= \frac{l_0^E}{\bar{v}}\frac{\alpha}{\alpha-1}\left((\alpha-1)c_o^{\alpha-1}P_M F\right)^{1/\alpha} + \frac{l_0^{NE}}{\bar{v}}\frac{\alpha}{\alpha-1}\left((\alpha-1)c_o^{\alpha-1}P_H F\right)^{1/\alpha} \\ &= \frac{\alpha}{(\alpha-1)\bar{v}}\left((\alpha-1)c_o^{\alpha-1}P_H F\right)^{1/\alpha}\left(l_0^E\left(\frac{P_M}{P_H}\right)^{\frac{1}{\alpha}} + l_0^{NE}\right) \end{aligned} \tag{4}$$

When l_0^{NE} vanishes to zero, the total cost C_0 without evasion behavior only includes the part inside ECA.

Recall that the optimal sailing speed is independent on the length of trajectory segments. Therefore, by substituting l_0^E and l_0^{NE} to l^E and l^{NE}, the sailing speeds inside and outside ECA with evasion behavior can be calculated by Eqs. (2) and (3), respectively. Given l^E and l^{NE}, the total cost of a ship with evasion behavior can also be expressed by Eq. (4). According to our assumption that the evasion trajectory is shifted to the right-hand side of the initial trajectory with a larger length, and we must have $l^E + l^{NE} \geq l_0^E + l_0^{NE}$. The problem of a ship

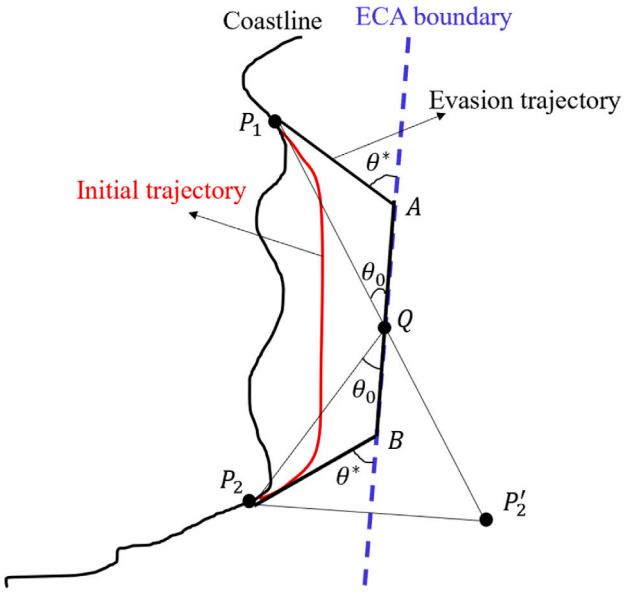

Fig. 3. Determination of optimal evasion trajectory.

to select the evasion trajectory under regulation of ECA is equivalent to the following minimization problem

$$\min_{\mathcal{J}} \left(\frac{P_M}{P_H}\right)^{1/\alpha} l^E + l^{NE} \tag{5}$$

subject to

$$l^E + l^{NE} \geq l_0^E + l_0^{NE} \tag{6}$$

We move to investigate the solution of Problem (5) and (6) or determine the evasion trajectory for a coastal ship under regulation of ECA. We first consider case (a) when the initial trajectory completely locates inside ECA, shown as Fig. 2(a). In this case, $l_0^{NE} = 0$. For the first plot the symmetric points of one port about the boundary Γ, and determine the shortest line by connecting the symmetric point with another port. The shortest line intersects with the boundary Γ at point Q, then the sum of lengths of $\overline{PQ}$ and $\overline{QP'}$ is shortest. The intersection angles of $\overline{PQ}$ and $\overline{QP'}$ with Γ are equal, denoted by θ_0. Observing the objective function of Problem (5), we know that, if $\cos\theta_0 > \left(P_H/P_M\right)^{1/\alpha}$, then it is better to decrease the length of l^E and increase l^{NE} since the total cost decreases. Otherwise, the ship cannot save its cost with evasion strategy. The optimal locations A and B such that both intersection angles of $\overline{PA}$ and $\overline{BP'}$ with Γ are equal, denoted by θ^* with $\cos\theta^*$ is exactly equal to $\left(P_H/P_M\right)^{1/\alpha}$. When the piecewise line $PABP'$ locates in the right-hand-side area of initial trajectory $\mathcal{J}_0$, then piecewise line $PABP'$ is the optimal evasion trajectory $\mathcal{J}$. Fig. 3 shows a graphical explanation of determining the optimal evasion trajectory.

Let d_0 denote the sum of the distances between the ports P, P' and ECA boundary Γ. With θ^* and θ_0, l^E and l^{NE} can be calculated by

$$l_E = \frac{d_0}{\sin\theta^*} \tag{7}$$

and

$$l_{NE} = d_0\left(\cot\theta_0 - \cot\theta^*\right) \tag{8}$$

Substituting l^E and l^{NE} into Eq. (4), we have

$$C = \left[\frac{\alpha}{(\alpha-1)\bar{v}}\left((\alpha-1)c_o^{\alpha-1}P_H F\right)^{1/\alpha}\right] d_0\left(\tan\theta^* + \cot\theta_0\right) \tag{9}$$

Comparing C_0 given by Eq. (4) with $l_0^{NE} = 0$ and C given by Eq. (9), we know that, a ship considers an evasion trajectory if and only if $C_0 \geq C$, namely,

$$\begin{aligned} C_0 \geq C &\Leftrightarrow l_0^E\left(\frac{P_M}{P_H}\right)^{1/\alpha} \geq d_0\left(\tan\theta^* + \cot\theta_0\right) \\ &\Leftrightarrow \frac{l_0^E}{\Pi_\Gamma(\mathcal{J}_0)} \geq \cos\theta^* + \sin\theta^*\tan\theta_0 \end{aligned} \tag{10}$$

where $\Pi_\Gamma(\mathcal{J}_0)$ is the length of the projection of initial trajectory $\mathcal{J}_0$ on the ECA boundary Γ. The condition means that the arc length of the initial trajectory is not too long in comparison with its projection on the ECA boundary, the ship should not choose evasion strategy under ECA regulation. Otherwise, the ship should consider to sail along the ECA boundary.

Different from Fagerholt et al. (2015) and Wang and Peng (2019), we show a general condition for a coastal ship to choose evasion strategy. To build a relation with their results of Fagerholt et al. (2015) and Wang and Peng (2019), we can also set assume that the trajectory is a line parallel the ECA boundary. In this case, the first term of the last inequality of (10), $\frac{l_0}{\Pi_\Gamma(\mathcal{J}_0)} = 1$ since $\Pi_\Gamma(\mathcal{J}_0) = l_0$. As a result, the ship wants to sail along the ECA boundary provided that

$$\frac{d_0}{l_0} = \tan\theta_0 < \frac{1-\cos\theta^*}{\sin\theta^*} = \tan\frac{\theta^*}{2} \tag{11}$$

The condition is not restrictive since the price of the MGO is always higher than that of HSFO. Given 12 nautical miles for the China' ECA boundary, under the ideal assumption, all ships with an arc length exceeding $24 \times \cot\frac{\theta^*}{2}$ nautical miles would choose to sail along the ECA boundary. We take α typically equal to 3. When the price of MGO is more than 10 percent than that of HSFO, the ships with distances exceeding 190 nautical miles will consider to sail along the ECA boundary, which includes almost all port pairs of China. Furthermore, when the ratio of prices of HSFO and MGO decreases, θ^* increases, and thus, $\cot\frac{\theta^*}{2}$ also decreases. More coastal ships tend to sail along the ECA boundary. Note that, in reality, $l_0 \gg \Pi_\Gamma(\mathcal{J}_0)$ because of the complicity of the coastline.

In the current study, ECA boundary is assumed to a line to simplify our theoretical analysis. It must be pointed out that, both the coastline and ECA boundary are not line, and thus, the distance between the coastline and ECA boundary is not fixed. To simplify our discussion, we assume that the sailing trajectories of ships are given before ECA policy. We assume that the evasion behavior of a ship is to adopt a new trajectory which is farther away from the coastline than the current trajectory does provided that the new trajectory results in a lower operation cost.

3.2. Simulation method for general case

Condition (10) derived in the previous subsection is restrictive which requires that the initial trajectory must locate completely inside ECA and the evasion trajectory obtained by the geometric method is completely located in the right-hand-side area of the initial trajectory. In this subsection, we proposed a simulation method for the general case based on three rules described: Rule 1, the evasion trajectory must locate completely the right-hand-side area of the initial trajectory; Rule 2, the intersection angle between the evasion trajectory and the ECA boundary must not less than θ^* with $cos\theta^* = (P_H/P_M)^{1/\alpha}$; Rule 3, only one entering and exiting points of outside ECA provided that an evasion strategy is selected by a ship.

To make the simulation evasion trajectory more practically reasonable, we construct the minimal convex hull of the initial trajectory satisfying the above three rules, shown as Fig. 4. For the case shown in Fig. 4(a), even though the initial trajectory completely locates inside ECA, however, the trajectory obtained from optimization problem (5) and (6) would not be feasible. As we have discussed in the previous subsections, the evasion trajectory must shift to the right side of the initial trajectory for the safety consideration since we assume that the initial trajectory is optimal one. Then, according to rules 1 to 3, the evasion trajectory is the minimal convex hull of the initial trajectory with minimal total length and piecewise line. Furthermore, the intersection of the piecewise line and the boundary is exactly equal to θ^*. For the case shown in Fig. 4(b), the initial trajectory passes through outside ECA, we can construct the convex hull of the initial trajectory. However, the ship cannot sail along the ECA boundary based on Rule 2. As shown in Fig. 4(b), if the angle of the original trajectory and ECA boundary is less than best course angle θ^*, the ship could adjust its trajectory and meet the angle θ^* to bypass ECA. The adjusted trajectory must be outside of the original trajectory, which means the adjusted trajectory is based on the envelope line of the original trajectory. In the simulation process, we first depicted the adjusted trajectory based on the best course angle. A common outline of the original trajectory and adjusted trajectory is then extracted as an evasion trajectory, which could be regarded as an envelope line. For the case shown in Fig. 4(c), the initial trajectory passes through outside ECA and the intersection between any tangent line passing the point on initial trajectory inside ECA and the ECA boundary exceeds θ^*. In this case, the ship cannot reduce its cost by evasion strategy, and the evasion trajectory is the same of the initial trajectory. After obtained the evasion trajectory, we can calculate the arc lengths l^E, l^{NE}, and the corresponding total cost C according to Eq. (4). The evasion behavior happens for a ship if and only if $C < C_0$.

3.3. Efficiency of ECA policy with evasion behavior of ships

The evasion behavior of coastal cargo ships has a significant effect on both total transportation cost along the coastline and the total emission on the coastal area. It is clear to see that the evasion behavior reduces the operation cost of ships, and thus the total transportation cost along the coastline. However, the evasion behavior would distort the expectation of policy maker since the ships would sail outside ECA with HSFO. With the sailing speeds, arc lengths inside and outside ECA under evasion strategy of a ship, the pollution emission of a ship is the production of the fuel consumption and emission factor. In this paper, we only focus on the pollutant of SO_x of a ship with only one trip. It is easy to calculate the annual emission for a ship by multiplying its annual trip number. The emission of a ship with evasion behavior and only one trip is now calculated by

$$\mathcal{E} = \beta_M F\frac{l^E}{v^E}\left(\frac{v^E}{\bar{v}}\right)^\alpha + \beta_H F\frac{l^{NE}}{v^{NE}}\left(\frac{v^{NE}}{\bar{v}}\right)^\alpha \tag{12}$$

where β_M and β_H are the emission factors of different air pollutants with MGO and HSFO with $\beta_M < \beta_H$, such as CO_2, SO_x; v^E, l^E and v^{NE}, l^{NE} are the sailing speeds and arc lengths inside and outside ECA. Substituting the sailing speeds inside and outside ECA determined by Eqs. (2) and (3) into Eq. (12) gives rise to

$$\mathcal{E} = \frac{F}{\bar{v}}\left(\frac{c_o}{(\alpha-1)P_H F}\right)^{1-1/\alpha}\left\{\beta_M l^E\left(\frac{P_H}{P_M}\right)^{1-\frac{1}{\alpha}} + \beta_H l^{NE}\right\} \tag{13}$$

Note that $\beta_H > \beta_M$ for MGO and HSFO. When a ship considers an evasion strategy or problem (5) and (6), l^E tends to decrease and l^{NE} tends to increase. Denote $\mathcal{E}_0$ as the emission without evasion

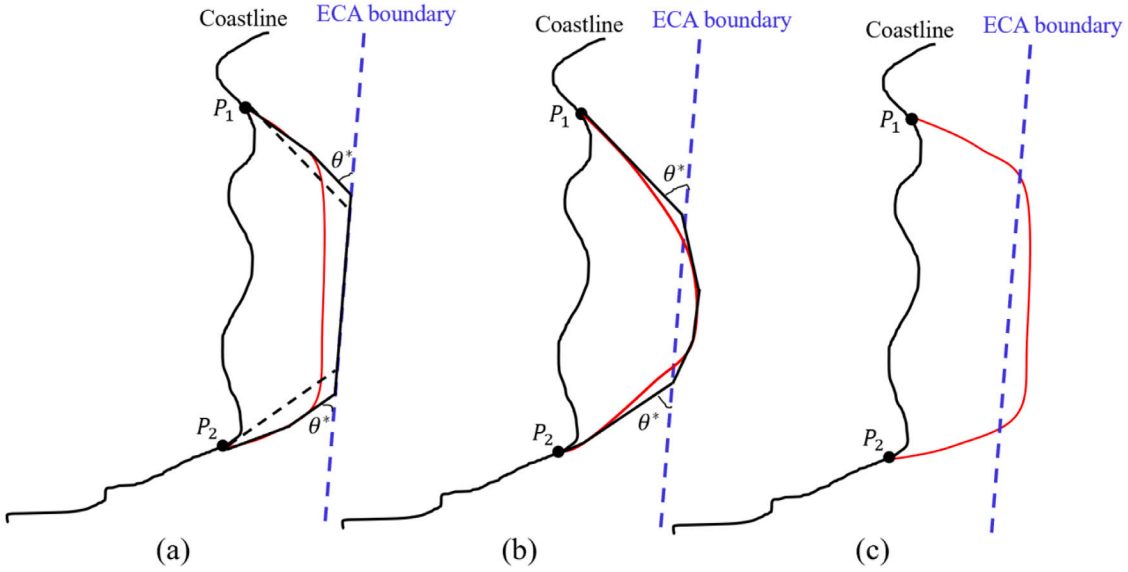

Fig. 4. Construct the evasion strategy with proposed simulation method.

behavior. Given a ship, the rate of the emission with and without evasion behavior can be calculated by

$$\begin{aligned}\frac{\mathcal{E}}{\mathcal{E}_0} &= \frac{\beta_M l^E \left(\frac{P_H}{P_M}\right)^{1-\frac{1}{\alpha}} + \beta_H l^{NE}}{\beta_M l_0^E \left(\frac{P_H}{P_M}\right)^{1-\frac{1}{\alpha}} + \beta_H l_0^{NE}} \\ &= \frac{\left(\frac{P_M}{P_H}\right)^{\frac{1}{\alpha}} l^E + l^{NE} - \left(1-\frac{\beta_M}{\beta_H}\frac{P_H}{P_M}\right)\left(\frac{P_M}{P_H}\right)^{\frac{1}{\alpha}} l^E}{\left(\frac{P_M}{P_H}\right)^{\frac{1}{\alpha}} l_0^E + l_0^{NE} - \left(1-\frac{\beta_M}{\beta_H}\frac{P_H}{P_M}\right)\left(\frac{P_M}{P_H}\right)^{\frac{1}{\alpha}} l_0^E} \\ &= \frac{C - \left(1-\frac{\beta_M}{\beta_H}\frac{P_H}{P_M}\right)C^E}{C_0 - \left(1-\frac{\beta_M}{\beta_H}\frac{P_H}{P_M}\right)C_0^E} \\ &= \frac{C^{NE} + \frac{\beta_M}{\beta_H}\frac{P_H}{P_M}C^E}{C_0^{NE} + \frac{\beta_M}{\beta_H}\frac{P_H}{P_M}C_0^E}\end{aligned} \tag{14}$$

where C_0^E and C^E are the costs inside ECA without and with evasion behavior, and correspondingly, C_0^{NE} and C^{NE} are the costs outside ECA without and with evasion behavior. According to relationship (14), we know that

$$\frac{\mathcal{E}}{\mathcal{E}_0} \le 1 \Longleftrightarrow \frac{C^{NE} - C_0^{NE}}{C_0^E - C^E} \le \frac{\beta_M}{\beta_H}\frac{P_H}{P_M}. \tag{15}$$

Condition (15) implies that it is not always bad for the evasion behavior. When the cost increase of a ship outside ECA caused by its evasion behavior is not too large and satisfy the second inequality of condition (15), the emission is also decreasing. However, the condition is practically restrictive since the emission factor of MGO is quite smaller than that of HSFO, while its price is very higher than that of the latter.

4. Case study between Ningbo and Xiamen ports

In this section, we take the coastal cargo ships traversing between Ningbo and Xiamen ports as an example, shown in Fig. 5. Based on the real trajectories of ships extracted from the Automatic Identification System (AIS) data, we first analyzed the evasion behavior of ships according to the simulation method proposed in Section 3, and then, investigated the effects of the size of ECA on the evasion behavior of ships and corresponding cost and emission between the two ports.

Table 2
Fuel parameters.

	HSFO	MGO
Price (USD/mt)[a]	392.50	619.00
Emission Factor (SO_2)[b]	0.054	0.001

[a]Data Source: https://bunkerindex.com/.
[b]Data Source: IMO GHG Study (2009).

Table 3
Containership T/C-Rates (USD per TEU per day)[a].

Ship size	Rates	Ship size	Rates
1100	8.30	3500	5.74
1700	7.76	4250	5.72
2500	6.74	5700	5.44
2700	6.94	6500	5.10

[a]Data Source: https://www.vhbs.de/index.php?id=13&L=1.

An efficiency assessment of the ECA policy with evasion behavior is discussed.

4.1. Data description

The AIS data from May to July 2019 is adopted to obtain the real trajectories of all coastal cargo ships, sailing speeds and fuel consumption rates. The AIS data is available on the website: http://www.shipdt.com/. The prices of the MGO and HSFO fuels' prices are 619.00 USD/mt and 392.50 USD/mt, obtained from http://www.zsbunker.cn. The emission factors of MGO and HSFO is 0.001, 0.054, respectively. These parameter are listed in Table 2

To estimate the ship's operation ratio, we investigated the container ship's hire fee from VHBS, a professional ship charter company. The ship's chartering cost is related to the number of containers on the ship, so the chartering cost of the whole ship can be spread evenly to each container. The website gives a single container rental cost for different types of ships, as shown in Table 3.

The original data from AIS is constructed by discrete points of ships on the map, and these trajectories have made their optimal decision under the current ECA policy. Some trajectory is mussy, such as circling or with too large course angle when turn direction. These abnormal points are removed from the trajectory, and some new points are complemented. A set of line segments forms China's ECA boundary, and

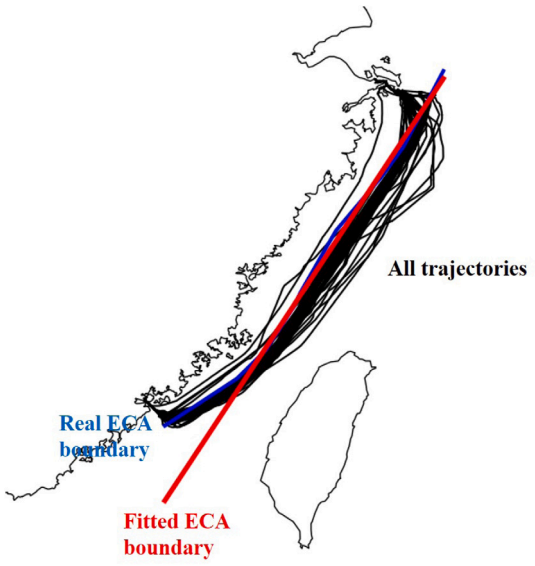

Fig. 5. ECA boundary and trajectories from Ningbo Port to Xiamen Port.

the ECA boundary between Ningbo Port and Xiamen Port is near a line. The fitted ECA boundary and processed trajectories are shown in Fig. 5.

4.2. Evasion behavior of ships

We investigate the trajectory's evasion behaviors under different ECA distance. Fig. 6 from (a) to (d) give ships' decision under ECA distance with 12 nm, 42 nm, 46 nm and 72 nm respectively. The evasion trajectory is figured by the red line. In Fig. 6(a), there only one trajectory that chooses to give up its old trajectory and choose evasion strategy. There have two reasons to drive this outcome. First, the data we used is extracted from 2019, so these ships have made the best decision under the current ECA policy. The second reason is that the current ECA boundary is too close to the coastline, and most of the trajectories have passed by ECA. With ECA distance moving far away from the coastline, the adjusted trajectories increase and decrease gradually. The adjusted ratio is increased and decreased with ECA distance moving from 12 nm to 72 nm. At the same time, the total distance of all trajectories is also increasing and decreasing. At the beginning of ECA moving, most trajectories have escaped the ECA boundary, so the adjusted ratio is low. With the ECA boundary moving outside of most trajectories, it is not very hard for these ships to bypass the ECA boundary. However, with the ECA boundary moving, the distance between the old trajectory and ECA boundary increases, becoming more expensive for ships to pass the ECA boundary. This is the reason the adjusted ratio decrease slowly. In the end, when ECA distance is set to 72 nm (very far from the coastline), there is no ship choose evasion strategy.

We suppose the ship use MGO in ECA and burn HSFO outside ECA. The total emission of sulfide of one trajectory is divided into inside ECA and outside ECA. Based on the trajectory of ships, we calculate its emission inside the ECA and outside the ECA under different ECA distance. Furthermore, the total cost and the total emission before and after ships choose evasion strategy are shown in Fig. 7. The Δ_1 is the total cost gap before and after ships choose evasion trajectories. The Δ_2 is the total emission gap before and after ships choose evasion trajectories. Fig. 7 shows that the saved cost Δ_1 is increases and decreases with the ECA boundary moving. On the other hand, the retard emission also increases and decreases with ECA boundary changes. The ship could save the cost by evasion strategy to pass by ECA, but this behavior retard the emission regulation simultaneously. Moreover, although the total emission decreases with the ECA move, the decrease ratio is different under different ECA distance. With the ECA boundary moving far away from the coastline, the number of ships choose evasion strategy increase, and the emission reduction is retarded. When ECA boundary moves to 48 nm, the cost of evasion strategy becomes expensive, and more ship chooses to comply with ECA regulation. In this case, the emission reduction becomes significant. When the ECA boundary is set to 72 nm, all trajectories will not choose to pass by the ECA boundary because the evasion strategy is too expensive. Moreover, the emission gets a minimum value. The yellow line in Fig. 7 is the current ECA (12 nm). In this regulation, the Δ_1 and Δ_2 are little, and the emission reduction compared with no ECA policy is less.

4.3. Efficiency of the ECA policy

Furthermore, to more evidently obvious about the relationship between the reduction emission and reduction of cost. We define the efficiency rate as $e = \frac{\Delta_{emission}}{\Delta_{cost}}$, which means how many kilograms of sulfur emissions are reduced for unit operation cost increased. The changes of value e with the ECA distance change is shown in Fig. 8. The overall trend of e is decreasing and increase then. The value of e in the start is lower than the middle, because the ship could choose the evasion strategy to pass by the ECA to slow down emission reduction. However, the value of e gets a peak when ECA is around 54 nm. The reason caused this result is that when ECA is moving far away from the coastline, more than 42 nm, the evasion strategy is become more and more expensive. So, more and more ships choose to comply with the ECA policy and sailing inside the ECA. If the ship chooses sailing inside the ECA, the emission reduction is great because the ratio of sulfide of MGO and HSFO is considerable.

Furthermore, The line-source pollution emission model is improved to investigate the air pollution spread from ship to coastline (Fushimi et al., 2005; Cao et al., 2020; Yang et al., 2020). The ship's trajectory in the ocean could be regarded as a liner pollution source. This model could evaluate the emission density, which is spread to the shore. There have some parameters that need to input into this model. We assume the wind speed in the ocean is 25 m/s, and the high of the ship's chimney is 20 m. We calculated the received emission in the coastline in 15 m up in the air.

We focus on the ship's emission out of ECA burning HSFO. The gas pollution of SO_2 reach the coastline is listed in Table 4. The column *Distance* determines the distance between the trajectory and coastline. The column *Length* denotes the average sailing distance of ships out of the ECA. The Q means the emissions intensity for the liner pollution source. The last column indicates the concentration of SO_2 received on the shore. We could find the sailing distance outside of the ECA is gradually decreasing with the ECA distance increase. Moreover, the emission spread to the coastline decreases with ECA boundary moving, which is synchronous with shown in Fig. 8. The emission heat map changing from 12 and 72 nm are given to observe the emission changes under different ECA distance in Fig. 9. The reduced emission is conspicuous if the ECA boundary is far enough.

We investigated the Sulfur emission under different ECA boundaries, including the current ECA boundary of 12 nm. We also evaluated the emission result if the ECA enlarge to 72 nm under the evasion strategy. Fig. 7 in the paper shows that the emission reduction value under the current ECA boundary is relatively less than no ECA, just about 14%. If the ECA boundary enlarges to near 54 nm, the emission reduction is almost 85%, which is significant. However, the ship's cost is also increased with the ECA boundary moving far away from the coastline. Because the ship is required to use expensive MGO in the ECA, the government could trade off the relationship between emission reduction and ship cost increase. The global Sulfur emission limit is adjusted to 0.5% from 2020, consistent with China's ECA policy. But in the actual operation for ships near the coastline. Some ships would

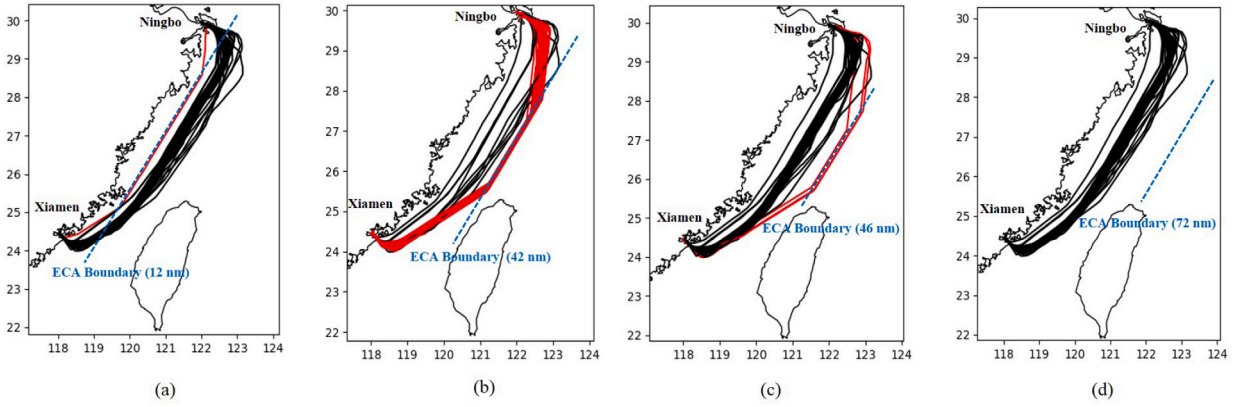

Fig. 6. The trajectories' behavior under different ECA boundary.

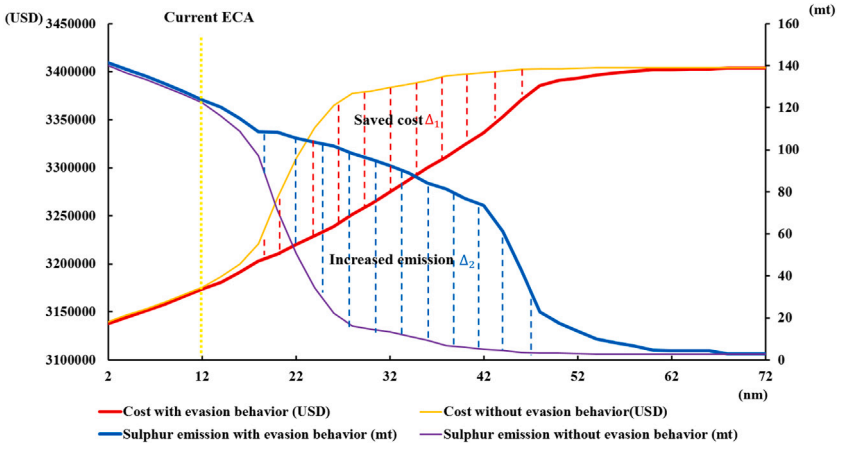

Fig. 7. The total cost and emission before and after ships choose evasion strategy under different ECA distance.

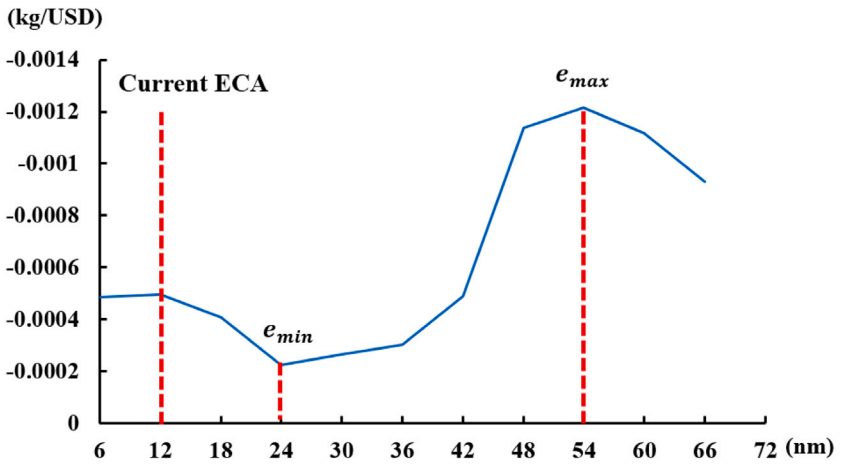

Fig. 8. The efficiency of emission reduction based on ship's cost increase under different ECA distance.

violate the regulation of the IMO. There are still some ships that use HSLO fuel offshore.

In the current study, the ship's behavior under different ECA policies was evaluated, which provided suggestions for the government to enlarge the ECA size. Previous studies mainly focused on the emission reduction affected by the ECA but seldom consider the ship's behavior. However, the evasion trajectory would retard the emission reduction effect. It must be pointed that the global Sulfur emission limit is adjusted to 0.5% from 2020, consistent with China's ECA policy. In theory, the ship does not need to bypass the ECA. However, in the real, by investigating, for some ships, they would not comply with the IMO regulation. The ship-owner still chooses to use heavy oil outside the ECA. So, it is still necessary for China's government to design its ECA. The research about the ship's behavior under ECA policy is also significant.

Compared to Wang and Peng (2019), our research considered a more realistic situation based on real AIS data, and the model we improved could handle non-parallel ports under ECA policy. Besides, the Wang and Peng (2019) only focused on the current ECA policy, and we investigated the ship's choices under different ECA distance. Li

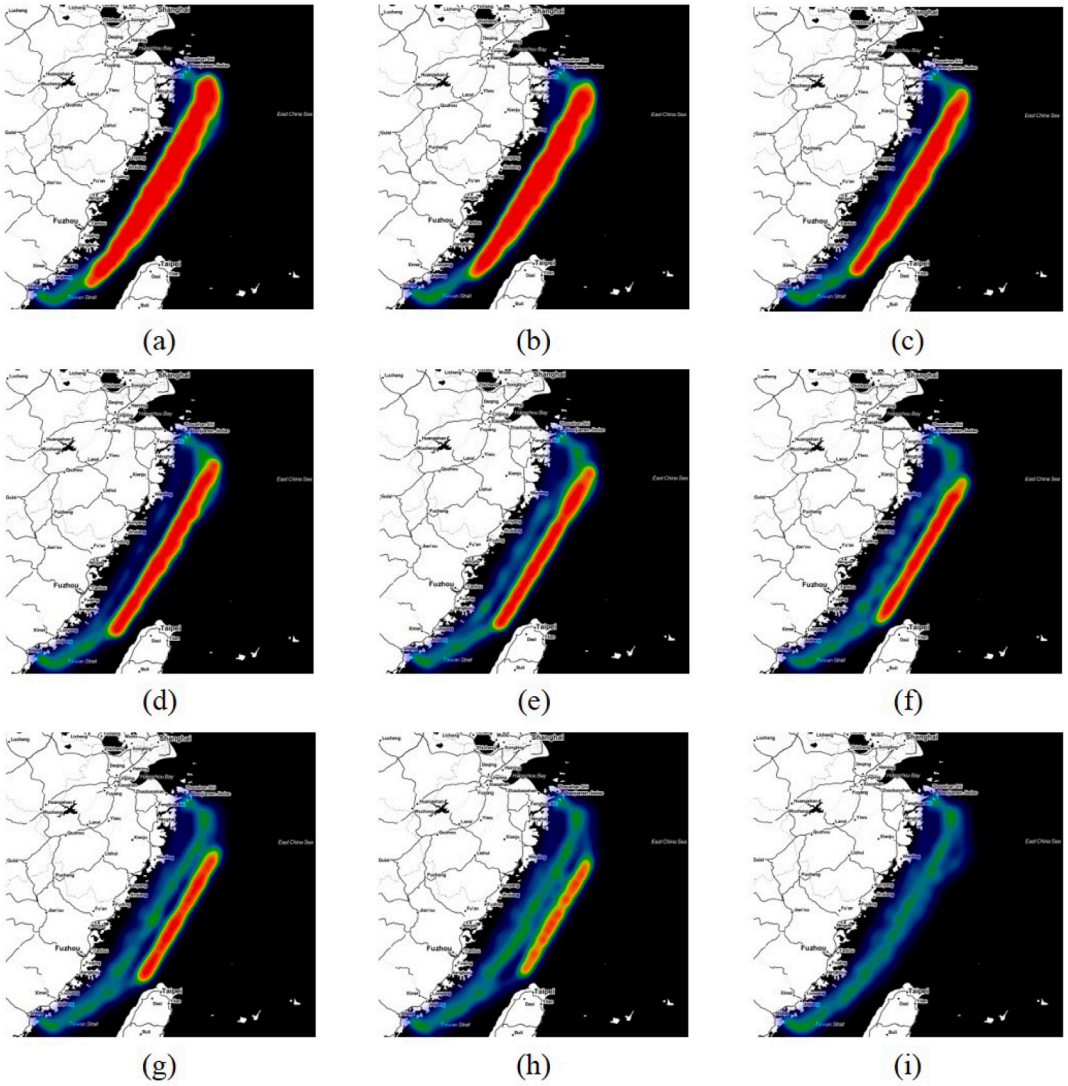

Fig. 9. The emission heat map under different ECA boundary.

Table 4
The concentration of SO_2 spread to the shore.

ECA (nm)	Distance (nm)	Length (nm)	Q(kg/s)	SO_2(ug/m^3)
12	12.18	168.37	8.50E−04	94.17
16	16.17	155.75	8.50E−04	75.94
20	20.28	147.86	8.50E−04	63.96
24	24.24	142.67	8.35E−04	54.84
28	28.23	135.67	8.35E−04	48.86
32	32.26	126.97	8.35E−04	44.14
36	36.29	118.86	8.09E−04	39.11
40	40.34	110.49	7.92E−04	35.33
44	44.40	101.66	6.73E−04	27.91
48	48.37	95.94	2.41E−04	9.37
52	52.39	97.06	1.31E−04	4.80
56	56.35	104.06	6.65E−05	2.30
60	60.32	97.30	2.26E−05	0.74
64	64.36	87.91	2.26E−05	0.71

et al. (2020) investigated the ship's behavior of two given ports under specific ECA boundary. They used an enumeration process to find the best position to enter and exit the ECA boundary. Furthermore, a non-linear mixed-integer model needs to be called frequently. In their study, the trajectories between two specific ports are homogeneous. However, the ships' evasion trajectories in our study are based on real AIS data, which is more practical. We given an analytical course angle if the ship chooses to pass ECA to sail. Furthermore, Li et al. (2020) found that the number of evasive ships will decrease from 39.05% to 29.05% after the fuel price ratio (MGO/LSFO) from 1.5 to 1.2. Our model could quickly achieve this conclusion. The value of θ^* become small if $\frac{P_H}{P_M}$ increase. This means the prices of these two fuels to be more closer. So fewer ships choose the evasion strategy.

5. Conclusions

Under the ECA policy, the ship will decide whether to choose the evasion strategy with different fuels to decrease its cost. This paper proposed a geometrical model to estimate the ship's behavior, dealing with the irregular coastline and irregular ship routes. The trajectory is described as a piecewise line, and the ports are not symmetric. There exists an optimal angle if the ship chooses to pass by ECA with different fuels. Based on this model, we simulated the ship's trajectory bypassing ECA using AIS data of 2019. Based on the mathematical model and three adjustment principles, a simulation method is presented. The simulation method and the geometrical model are used to calculate the old trajectory's cost and evasion trajectory's cost. The ship would choose the lower cost trajectory. It is easy to calculate the emission after we get the ship's decision. Under the current ECA policy, we

got only one adjusted trajectory because the ship has made its best decision under the current ECA policy. From another point of view, it proved the simulation method could depict the ship's behavior. Besides, the current ECA boundary is too close to the coastline, and it is not too expensive for them to pass by ECA. So, most ships have chosen to bypass ECA to sailing. However, with the ECA boundary moving far away to shore, the number of evasion trajectories increases first and decreases. In the meantime, the distance of total distance is also increasing and decreases gradually.

Some of our conclusions could also be supported by previous studies. Fagerholt et al. (2015) demonstrated that ship-owners could react in ways that may limit ECA's effectiveness. Most ships will choose an evasion strategy to reduce sailing inside the ECA with expensive fuel oil. Li et al. (2020) indicated that whether the ship chooses the evasion strategy is related to the fuel prices ratio, similar to θ^* in the current study. Moore et al. (2018) documented decreased speeds in the ECA and increased speeds outside of the ECA by AIS data.

Furthermore, with the ECA boundary moving, the ship's cost increases, and the total emission decreases. However, the reduction ratio of emission changes, and we give a detailed description of the caused reason. Moreover, we calculated the emission reduction ratio related to unit operation cost increase. We found the emission reduction efficiency is low when the ECA boundary is close to the coastline. Moreover, emission reduction efficiency decreases and increases then.

It must be pointed out that the current study assumes that the ECA boundary is a line and only considers the sailing behavior between two ports. However, in practice, the ECA boundary is always a piecewise line and there is a complicated shipping network connecting all the coastal ports. Therefore, to extend our model to consider the general shipping network and real ECA boundary is one of future research directions. Secondly, the sea environment or condition, such as ocean current, wave height, water and wind velocity, has a significant effect on the sailing behavior of ships. To develop the stochastic methodology to incorporate the uncertain factors is another research direction. Thirdly, shipping costs changes vary significantly across vessel categories (Gonyo et al., 2019). Multiple ship types, such as, cargo ships, cruises, fishing boats, should be considered since the ECA policy has different effects on those ships. Last but not least, it is necessary to build new model to study the effect and efficiency of ECA policies from different countries and regions.

Declaration of competing interest

The authors declare that they have no known competing financial interests or personal relationships that could have appeared to influence the work reported in this paper.

Acknowledgments

This study was supported by Research Fund of the National Natural Science Foundation of China (71871037, 71831002, 71471068).

References

Cao, B., Cui, W., et al., 2020. Development and uncertainty analysis of radionuclide atmospheric dispersion modeling codes based on Gaussian plume model. Energy 194, 116925.

Cariou, P., Cheaitou, A., et al., 2018. Liner shipping network design with emission control areas: A genetic algorithm-based approach. Transp. Res. D 63, 604–621.

Carr, E.W., Corbett, J.J., 2015. Ship compliance in emission control areas: technology costs and policy instruments. Environ. Sci. Technol. 49, 9584–9591.

Chen, L., Yip, T.L., et al., 2017. Provision of emission control area and the impact on shipping route choice and ship emissions. Transp. Res. D 58, 280–291.

Dong, G., Lee, P.T.W., 2020. Environmental effects of emission control areas and reduced speed zones on container ship operation. J. Clean Prod. 274, 122582.

Fagerholt, K., Gausel, N.T., et al., 2015. Maritime routing and speed optimization with emission control areas. Transp. Res. C 52, 57–73.

Freedman, R., Herron, S., et al., 2017. The effectiveness of incentivized and non-incentivized vessel speed reduction programs: case study in the santa barbara channel. Ocean Coast. Manage 148, 31–39.

Fushimi, A., Kawashima, H., et al., 2005. Source apportionment based on an atmospheric dispersion model and multiple linear regression analysis. Atmos. Environ. 39, 1323–1334.

Gonyo, S.B., Goedeke, T.L., et al., 2019. An economic analysis of shipping costs related to potential changes in vessel operating procedures to manage the co-occurrence of maritime vessel traffic and whales in the channel islands region. Ocean Coast. Manage 177, 179–187.

International Maritime Organization, 2021. Prevention of air pollution from ships. https://www.imo.org/en/OurWork/Environment/Pages/Air-Pollution.aspx.

Jiang, B., Wang, X., et al., 2020. An evolutionary game model analysis on emission control areas in China. Mar. Pol. 118, 104010.

Kong, Y., Liu, J., 2021. Sustainable port cities with coupling coordination and environmental efficiency. Ocean Coast. Manage 205, 105534.

Li, L., Gao, S., et al., 2020. Ship's response strategy to emission control areas: from the perspective of sailing pattern optimization and evasion strategy selection. Transp. Res. E 133, 101835.

Ma, W., Lu, T., et al., 2020a. Ship route and speed multi-objective optimization considering weather conditions and emission control area regulations. Marit. Policy Manag. 1–16.

Ma, D., Ma, W., et al., 2020b. Method for simultaneously optimizing ship route and speed with emission control areas. Ocean Eng. 202, 107170.

Meng, Q., Du, Y., Wang, Y., 2016. Shipping log data based container ship fuel efficiency modeling. Transp. Res. B 83, 207–229.

Ministry of Transport of the People's Republic of China, 2018. https://xxgk.mot.gov.cn/2020/jigou/haishi/202008/t20200828_3457437.html.

Mollenbach, C.K., Schack, C., et al., 2012. Vessel Emission Study: Comparison of Various Abatement Technologies to Meet Emission Levels for ECA's. Tech. Rept.

Moore, T.J., Redfern, J.V., et al., 2018. Exploring ship traffic variability off California. Ocean Coast. Manage 163, 515–527.

Okada, A., 2019. Benefit, cost, and size of an emission control area: a simulation approach for spatial relationships. Marit. Policy Manag. 46, 1–20.

Pawlak, M., 2015. Analysis of economic costs and environmental benefits of LNG as the marine vessel fuel. Trans. Tech. Publ. Ltd 236, 239–246.

Peng, Y., Li, X., et al., 2019. A method for determining the allocation strategy of on-shore power supply from a green container terminal perspective. Ocean Coast. Manage 167, 158–175.

Peng, Y., Wang, W., et al., 2016. A stochastic seaport network retrofit management problem considering shipping routing design. Ocean Coast. Manage 119, 169–176.

Ronen, D., 1982. The effect of oil price on the optimal speed of ships. J. Operat. Res. Soc. 33, 1035–1040.

Shi, K., Weng, J., et al., 2020. Exploring the effectiveness of ECA policies in reducing pollutant emissions from merchant ships in Shanghai port waters. Mar. Pollut. Bull. 155, 111164.

Tan, Z., Wang, Y., Meng, Q., Liu, Z., 2018. Joint ship schedule design and sailing speed optimization for a single inland shipping service with uncertain dam transit time. Transp. Sci. 52, 1297–1588.

UNCTAD, 2017. Review of Maritime Transport. United Nations, New York and Geneva.

UNCTAD, 2020. Review of Maritime Transport. United Nations, New York and Geneva.

Viana, M., Fann, N., et al., 2015. Environmental and health benefits from designating the marmara sea and the turkish straits as an emission control area (eca). Environ. Sci. Technol. 49, 3304.

Wan, C., Yan, X., et al., 2019a. An advanced fuzzy bayesian-based fmea approach for assessing maritime supply chain risks. Transp. Res. E 125, 222–240.

Wan, C., Yan, X., et al., 2019b. Analysis of risk factors influencing the safety of maritime container supply chains. Int. J. Shipp. Transp. Logist. 11, 476–507.

Wang, S., Meng, Q., 2012. Sailing speed optimization for container ships in a liner shipping network. Transp. Res. E 48 (3), 701–714.

Wang, S., Peng, C., 2019. Model and analysis of the effect of China's potential domestic emission control area with 0.1% sulphur limit. Marit. Busi. Rev. 4, 298–309.

Wang, Z., Zhao, L., et al., 2020. An empirical correlation mechanism of economic growth and marine pollution: a case study of 11 coastal provinces and cities in china. Ocean Coast. Manage 198.

World Shipping Council, 2021. https://www.worldshipping.org/.

Yang, Z., Yao, Q., et al., 2020. Modification and validation of the Gaussian plume model (GPM) to predict ammonia and particulate matter dispersion. Atmos. Pollut. Res. 11 (7), 1063–1072.

Yu, J., Ma, J., et al., 2020. Historical evolution of marine functional zoning in china since its reform and opening up in 1978. Ocean Coast. Manage 189.

Zhang, Q., Zheng, Z., et al., 2020. Does emission control area policy reduce sulfur dioxides concentration in shanghai?. Transp. Res. D 81, 102289.

Zhen, L., Li, M., et al., 2018. The effects of emission control area regulations on cruise shipping. Transp. Res. D 62, 47–63.

Zheng, H., Zhang, J., et al., 2020. Exploring the affecting mechanism between environmental regulation and economic efficiency: New evidence from China's coastal areas. Ocean Coast. Manage 189, 105148.